Modelling Development of Epidemics with Dynamic Small-World Networks

Jari Saramäki *, and Kimmo Kaski

Laboratory of Computational Engineering, Helsinki University of Technology, P.O. Box 9203, FIN-02015 HUT, Finland

Abstract

We discuss the dynamics of a minimal model for spreading of infectious diseases, such as various types of influenza. The spreading takes place on a dynamic small-world network and can be viewed as comprising short- and long-range spreading processes. We derive approximate equations for the epidemic threshold as well as the spreading dynamics, and show that there is a good agreement with numerical discrete time-step simulations. We then analyze the dependence of the epidemic saturation time on the initial conditions, and outline a possible method of utilizing the model in predicting the development of epidemics based on early figures of infected. Finally, we compare time series calculated with our model to real-world data.

Key words:
epidemiology, spreading models, complex networks, infectious diseases

1 Introduction

Traditionally, mathematical models for the spread of a disease have relied on differential equations, describing the dynamics of spreading within uniformly mixed populations (Bailey, 1975; Anderson and May, 1991; Murray, 2001). The basic premise of uniform mixing is that all individuals in a group are equally likely to become infected. The spreading process itself is then captured using compartments, i.e. individuals belonging to epidemiological classes such as susceptible (S), exposed (E), infective (I) and recovered (R), between which the flows of population are described with rate equations. Within this framework,

* Corresponding author.
Email address: jsaramak@lce.hut.fi (Jari Saramäki).

the simplest model is the widely-utilized SIR (Susceptible-Infected-Removed) model (see e.g. Anderson and May, 1991; Hethcote, 2000), in which susceptible individuals may become infected and continue to infect others until finally removed from the system due to recovery, death, or containment.

The apparent shortcomings of the uniform mixing hypothesis have long been realized, and spatial effecs and heterogeneity have been show to have profound effects on the transmission, persistence and evolution of diseases (Mollison, 1977; Rand et al., 1995; Lloyd and May, 1996; Rhodes and Anderson, 1996; Keeling, 1999; Grenfell et al., 2001). Partially owing to the recent advances in the science of complex networks (Albert and Barabási, 2002; Dorogovtsev and Mendes, 2002; Newman, 2003), there has been increased interest in trying to capture the effects of contact patterns between individuals instead of relying on mean-field models. These patterns can be described using *contact networks*, where the vertices correspond to individuals and the edges to contacts between them (Wallinga et al., 1999). One of the major motivations for studying complex networks has been to better understand the structure of *social networks* (Watts and Strogatz, 1998; Girvan and Newman, 2002). As the structure of social networks, without a doubt, has to be reflected in contact networks, there is a natural link between epidemiological modeling and the science of complex networks.

The network approach to epidemiological modeling has proven to be fruitful in the context of the spreading dynamics of human disease as well as electronic viruses (Watts and Strogatz, 1998; Keeling, 1999; Boots and Sasaki, 1999; Newman, 2002; Pastor-Satorras and Vespignani, 2001; May and Lloyd, 2001; Read and Keeling, 2003; Meyers et al., 2003, 2005), yielding much insight on the mechanisms of disease spreading. Overall, the types of network structures used in these models can be divided into two categories: the so-called *small-world* and *scale-free* networks. A well-known result of these studies is that biological and computer viruses spread rapidly on both types of networks, which is mainly due to the very short average vertex-to-vertex distances along the links of the networks. In addition, spreading is further accelerated in scale-free networks due to a broad power-law distribution of connections per individual - the few highly connected hubs then act as "super-spreaders."

Generally, the term 'small-world network' refers to networks where a small number of shortcuts is introduced on a regular underlying lattice, either by adding new links between randomly selected vertices or randomly rewiring a fraction of the links (Watts and Strogatz, 1998). In terms of population mixing, a small-world structure is analogous to a situation where there are clusters of connected individuals (social groups), which have contacts with "nearby" groups as well as "far-off" groups via the sparse long-range links. In the context of epidemiology, a small-world contact network structure has lately been found to emerge in large-scale simulations based on urban traffic,

census, land-use and population-mobility data (Eubank et al., 2004).

Here, our aim is to model the spreading dynamics of a randomly contagious disease, such as a common influenza. The basic idea is to capture the essential elements of the dynamics by utilizing the SIR mechanism on a dynamically changing small-world contact network. Related works on static and dynamic small-world models (Watts and Strogatz, 1998; Newman and Watts, 1999; Moore and Newman, 2000; Zekri and Clerc, 2001; Hastings, 2003; Masuda et al., 2004; Zhu et al., 2004) have shown among others the existence of a shortcut-density-dependent epidemic threshold as well as novel scaling properties. Our focus is explicitly on the spreading dynamics, i.e. the time-domain development of an epidemic, formulated in terms of rate equations derived for our particular model.

This article is organized such that first we shall describe the spreading model in terms of a probabilistic discrete time-step process. Next, we will address the issue of the epidemic threshold and derive necessary conditions for the epidemic to take off. This is followed by derivation of analytical equations for a special case of this model, where the probability of infection transmission between neighbouring infective and susceptible individuals is set to one. We will then discuss the dependence of the duration of an epidemic on the initial conditions and the system size, and utilize the results in an attempt to construct a method for predicting the development of an epidemic based on early time data. Finally, we will compare time series generated with the model to real-world data.

2 Discrete time-step SIR model on a dynamic small-world network

First, let us discuss our model for the contact network, through which the spreading occurs. As mentioned above, social networks as well as simulated contact networks display the small-world property, which means that "long-range" contacts between individuals result in short average distances along the edges of the network. These long-range contacts may be viewed either as infrequent contacts, or random encounters. In addition, these networks have a regular underlying structure, which may be interpreted as groups of people with regular contacts – e.g. friends or colleagues. To capture the essentials of such a network, we define the network as comprising a regular one-dimensional lattice with N vertices having a coordination number $2z$, with additional randomly occurring long-range links, whose configuration is constantly changing. Periodic boundary conditions are used. This network acts as the substrate for spreading (see Fig. 1) in our model. We may also view the spreading process as composed of two different processes: the short-range (SR) spreading process corresponds to passing the disease on to the nearest circle of persons, and the

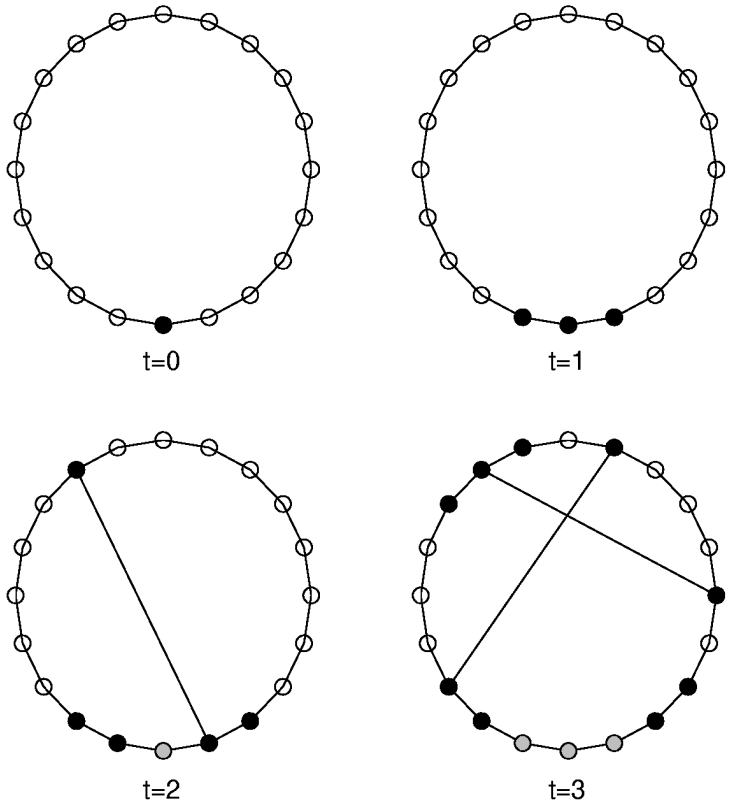

Fig. 1. Schematic of epidemic spreading on a dynamic small-world contact network with coordination number $2z = 2$. At time $t = 0$, a single vertex is infected (solid black circle). Then the infection spreads to neighbouring vertices ($t = 1$) as well as randomly chosen vertices ($t = 2$, $t = 3$). Recovered vertices are shown as solid grey circles.

long-range (LR) process to infecting any randomly encountered person.

The spreading itself is modeled using the SIR mechanism. All individuals in the network are at all times labeled as either susceptible (S), infected (I) or recovered (R). Initially, the status of $N - N_0$ individuals is set susceptible with N_0 individuals infected. The dynamics of the model are such that at every discrete time step of duration Δt, every infected individual in the network

(1) Infects its nearest neighbours, if susceptible, with probability p_s per neighbour,
(2) With probability p_j tries to infect one randomly chosen individual, succeeding if the individual is susceptible,
(3) With probability p_r recovers and can no longer be infected or infect others.

This process can be readily iterated in numerical simulations until changes no longer happen. The process step (1) corresponds to transmission of infection along the regular underlying lattice (the short-range process) and step (2)

amounts to the randomly changing long-range connections (the long-range process).

3 Analytical description

3.1 The epidemic threshold

First, we will derive the necessary conditions for an epidemic to take off, i.e. the epidemic threshold. For simplicity, we will only consider the case $2z = 2$, so that each network vertex has two nearest neighbours. As the spreading process is stochastic in nature, we will describe it with average quantities, which should be interpreted as averages over several epidemics. Let $I(t)$ denote the average number of infected individuals at time t and $N'(t)$ the average number of individuals ever infected. Let us also define an auxiliary quantity $F(t)$, which denotes the average number of pairs of vertices where one vertex is infected and its nearest neighbour susceptible, i.e. the number of fixed edges along which a short-range transmission can happen. We will call $F(t)$ the amount of domain walls, as the short-range spreading process can be viewed as growth of "domains" of infected people with the "walls" of these domains moving with velocity p_s. Now it is straightforward to write down equations for the changes in $N'(t)$ and $I(t)$:

$$\frac{dN'(t)}{dt} = p_s F(t), \tag{1}$$

and

$$\frac{dI(t)}{dt} = p_s F(t) - p_r I(t). \tag{2}$$

Next, consider the dynamics of the domain walls. Domain walls are created by the long-range spreading "jumps", two walls per jump, and destroyed by collisions when two spreading domains merge, as well as in events where an infected individual recovers before transmitting the disease to one of its neighbours. The jumps originate from the infected individuals with probability p_j per individual, and succeed if the randomly chosen target is susceptible, the probability of which equals $[N - N'(t)]/N$. Now consider a situation where at $t = 0$ we have a small initial number I_0 of infected vertices. For small times t and large N, we can neglect the effect of domain wall collisions, and write

$$\frac{dF(t)}{dt} = 2p_j \frac{N - N'(t)}{N} I(t) - p_r \left[1 - p_s\right] F(t), \tag{3}$$

where the first term on the r.h.s. corresponds to the creation of spreading domains and the second term to the effect of vertices recovering before disease transmission. At early times t, we may approximate $N'(t)/N(t) \approx 0$. Combining Eqs. (2) and (3) and moving to scaled variables so that $i(t) = I(t)/N$ we get

$$\frac{d^2 i(t)}{dt^2} + p_r \left(2 - p_s\right) \frac{di(t)}{dt} - \left[2 p_s p_j - \left(1 - p_s\right) p_r^2\right] i(t) = 0. \tag{4}$$

This equation has an exponential solution with two real eigenvalues $\lambda_{1,2}$, where the second eigenvalue is always negative. If the first is positive, the epidemic will take off leading to exponential growth of the number of infected. This condition is satisfied if

$$p_j > \frac{p_r^2 (1 - p_s)}{2 p_s}. \tag{5}$$

The above equation illustrates that in our simplified picture a certain probability of long-range jumps is necessary for crossing the epidemic threshold. One should also note the close relation to the corresponding percolation threshold on fixed small-world networks (Newman and Watts, 1999), and the role of the recovery probability in our model.

Figure 2 illustrates the threshold long-range infection probability $p_{j,c} = p_r^2 \left(1 - p_s\right) / 2 p_s$ as function of p_s. The average recovery time was fixed to $1/p_r = 6$, so that $p_r = 0.167$. The solid line indicates values given by Eq. (5), and the open circles show results of numerical simulations. The numerical results were generated by simulating the discrete-time-step model on networks with $N = 150,000$ and $N_0 = 15$ and averaging the maximum obtained epidemic sizes $n_{max} = N'_{max}/N$ over 50 runs. The N_0 vertices whose status was initially set to infected were selected randomly. Taking the finite system size into account and following Newman and Watts (1999), we chose the numerical threshold values $p_{j,c}$ as the points where n_{max} exceeds 0.2.

Finally, a note on the basic reproductive number R_0, which is defined as the average number of secondary infections produced by one infected individual introduced into a susceptible population. Typically, the epidemic threshold is expressed in terms of this quantity, so that an epidemic will take off only if $R_0 \geq 1$. Likewise, the spreading dynamics are often seen to depend mainly on R_0. The shortcomings of this quantity outside the homogeneous mixing assumption have long been known, and corrections have been suggested to take into account the effects of more complex spreading models (see e.g. Anderson and May, 1991). However, in our case, the spreading dynamics cannot be solely determined by the number of secondary infections caused by an infected individual. The reason for this is that the effect of a secondary infection caused

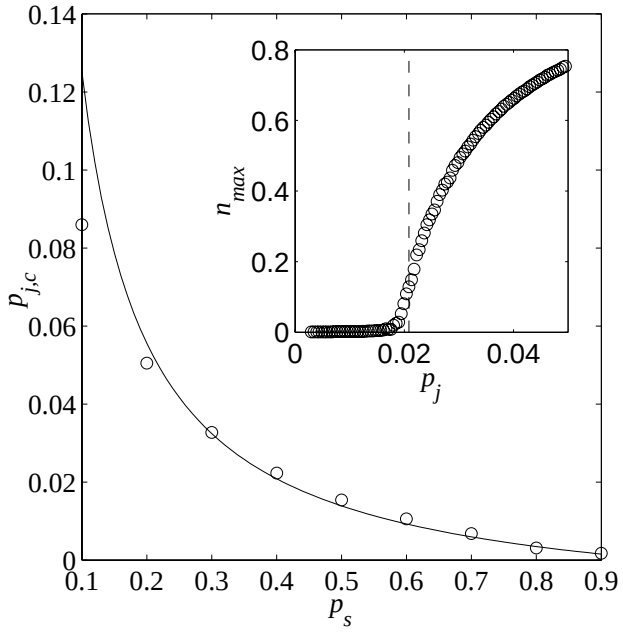

Fig. 2. Numerical results for threshold long-range probabilities $p_{j,c}$ (circles) on networks of size $N = 150,000$, with $N_0 = 15$ and $p_r = 0.167$. The solid line indicates the analytic approximation to $p_{j,c}$. Inset: an example simulated data series, displaying the average maximum epidemic size n_{max} as function of p_j for $p_s = 0.4$. The dashed line indicates the analytic approximation for the threshold.

by nearest-neighbour transmission is different from the one caused by a long-range jump. Especially at the beginning stages of the disease, long-range jumps will (almost) always generate new spreading domains expanding at rate $2p_s$ (or $\sim 2p_s z$, if we consider larger neighbourhoods), whereas nearest-neighbour transmissions only expand existing domains. Hence, the spreading dynamics depends on *who* will become infected in addition to how many such infections take place. This is somewhat intuitive - passing the disease on to "virgin territory" among susceptibles is likely to accelerate disease spreading more than transmission within a community, where the amount of susceptibles is already reduced.

3.2 Dynamics in the limit $p_s = 1$

Now, let us discuss a special case of the above spreading process, where we consider the nearest-neighbour spreading probability p_s to be unity so that before recovery happens, the nearest neighbours will always become infected. This restriction makes an analytical treatment of the dynamics of the model tractable. In this case, the epidemic will eventually cover the whole network of individuals. Considering the network to represent the whole susceptible population is clearly not a realistic assumption. However, we can conjecture

that a model where we *a priori* define the vertices of the network to represent only those individuals who at some point *will become* infected still represents the spreading dynamics adequately enough. In this case, N is to be viewed as the total epidemic size instead of the susceptible population size.

We will now derive analytical equations for the spreading dynamics based on the domain wall approach discussed in the previous section. Although the derivation assumes that $p_s = 1$, we will still retain the parameter in our formulas for reasons discussed below. Eqs. (1,2) still hold in the present framework, and we only have to rewrite the equation describing the domain wall dynamics. The domain wall creation term remains the same, but now the walls are destroyed by domain merging alone, and we need a term describing the rate of this annihilation process. At any time, the network contains $F(t)/2$ connected domains of susceptibles, containing altogether $N - N'(t)$ susceptible individuals. These domains "shrink" at velocity $2p_s$ due to the moving walls. The average domain length is $2\left[N - N'(t)\right]/F(t)$, and the average lifetime $\left[N - N'(t)\right]/\left[F(t)p_s\right]$. Two walls are destroyed per collision, and since there are $F(t)/2$ domains, on the average $p_s F(t)^2/\left[N - N'(t)\right]$ walls will be destroyed per unit time. Thus, we may write

$$\frac{dF(t)}{dt} = 2p_j \frac{N - N'(t)}{N} I(t) - p_s \frac{F(t)^2}{N - N'(t)}. \tag{6}$$

Now, we can again move to scaled variables $i(t) = I(t)/N$ and $n(t) = N'(t)/N$ and combine the above equations, arriving at

$$\frac{d^2 n(t)}{dt^2} + \frac{\left[dn(t)/dt\right]^2}{1 - n(t)} = 2p_s p_j \left[1 - n(t)\right] i(t), \tag{7}$$

$$\frac{di(t)}{dt} = \frac{dn(t)}{dt} - p_r i(t). \tag{8}$$

The system defined by Eqs. (7) and (8) can be solved by numerical iteration for both $n(t)$ and $i(t)$ using standard methods.

Figure 3 depicts the results of this numerical iteration and also the results of discrete time-step simulations, averaged over 100 runs. In these simulations, the network size was set to $N = 250,000$, the recovery probability per unit time to $p_r = 0.17$, and the spreading velocity to $p_s = 1$. The long-range jump probability was varied. The initial fraction of infected individuals was set to $n_0 = 25/250,000 = 1 \times 10^{-4}$. The fraction of individuals ever infected $n(t)$ is seen to follow an s-shaped curve such that in the beginning the fraction increases exponentially but then slows down to almost linear increase, as there is less and less susceptible population to be infected, and finally saturates as the epidemic covers the entire susceptible population. The theoretical curves

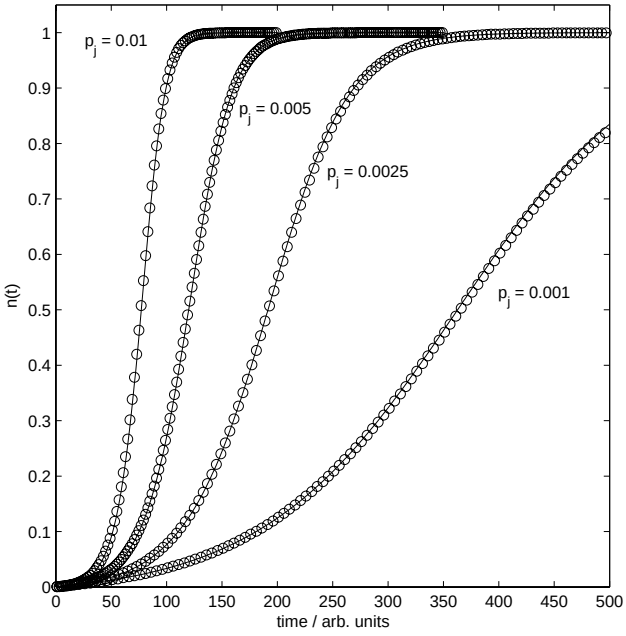

Fig. 3. The fraction of ever infected vertices n as function of time t calculated by simulated spreading on $N = 250,000$ networks (circles) and numerical integration of Eqs. (7) and (8) (solid lines), with nearest-neighbour spreading rate p_s=1, recovery rate p_r=0.17, and long-range jump probability p_j as illustrated. The results are averages over 100 runs.

calculated by numerical iteration of the above equations match the simulated results well.

Note that when $p_s < 1$, Eqs. (7) and (8) are still a good approximation to the system dynamics, as long as p_s is high enough to justify neglecting the effect of recovery-induced stopping of domain walls. Furthermore, should we wish to use larger neighbourhoods, we can simply absorb the coordination number into the definition on p_s so that $p_s \to p_s z$.

4 Scaling of the epidemic saturation time

Eqs. (7) and (8) indicate that the system size N enters the dynamics of the model only indirectly, in the form of the initial conditions $n_0 = N'(0)/N$. Hence, it is of interest to investigate the duration of the epidemic in networks of different sizes as a function of the initial density of infected n_0. Recently, it was shown that in a model where spreading takes place on small-world networks with dynamic rewiring of links and initial density of infected fixed to $n_0 = 1/N$, the epidemic saturation time depends on the network size as $\log N$ (Zhu et al., 2004).

Considering the practical use of such spreading models in e.g. predicting the development of an epidemic, a topic we will address shortly, setting the initial condition is somewhat problematic, as it is typically impossible to trace the beginning of an epidemic down to a single "patient zero". Hence, we have chosen to define the starting time of the epidemic in terms of an initial density of infected, such that at $t = 0$, $n(0) = n_0$, $n_0 \ll 1$. Furthermore, we define the saturation time t_f so that $t = t_f$ when $n(t) = n_f$, where we set n_f to a value somewhat less than unity. This "renormalization procedure" takes care of the asymptotic nature of the process both at its beginning and end.

Fig. 4 displays a log-linear plot of the saturation time t_f as function of n_0 for several network sizes N, ranging from 100,000 up to 800,000. The N_0 initially infected vertices were chosen randomly. Here, t_f was defined as the time when 95 % of the susceptible population has become infected, i.e. the first time step when $n(t) \geq 0.95$. The results of the simulations are taken as averages over 100 runs each, with $p_j = 0.008$, $p_r = 0.17$ and $p_s = 1$. The solid line depicts a fitted log-linear function, $t_f = -35.8 \times \log n_0 - 19.0$, showing a very good fit with the numerical results. It is evident that $t_f \propto -\log n_0$. This is in line with the $\log N$-scaling observed earlier with $n_0 = 1/N$ (Zhu et al., 2004), since $-\log n_0 = -\log N_0/N$ becomes $\log N$ when $N_0 = 1$.

The independence of the saturation time on the system size is further illustrated in the inset, which displays the fraction of individuals ever infected $n(t)$ averaged over 100 simulation runs of epidemics in networks of different size, with the initial condition $n_0 = 1 \times 10^{-4}$ and other parameters being $p_j = 0.005$, $p_r = 0.17$ and $p_s = 1$.

5 Method for predicting the development of an epidemic

Based on the above, we now outline a method for utilizing our model in predicting the future development of an epidemic from its early stages, where only a few data points of disease spreading exist. The accuracy of such predictions is naturally restricted by the simplifying assumptions we have used in constructing our model, as well as the apparent real-world limitations on data quality.

We start by approximating the system dynamics at early times t. Again, we set $p_s = 1$. Now, $n \approx 0$ and $(\partial n/\partial t)^2 \approx 0$ in Eq. (7), and we can write for $i(t)$

$$\frac{d^2 i(t)}{dt^2} + p_r \frac{di(t)}{dt} - 2p_j i(t) = 0. \tag{9}$$

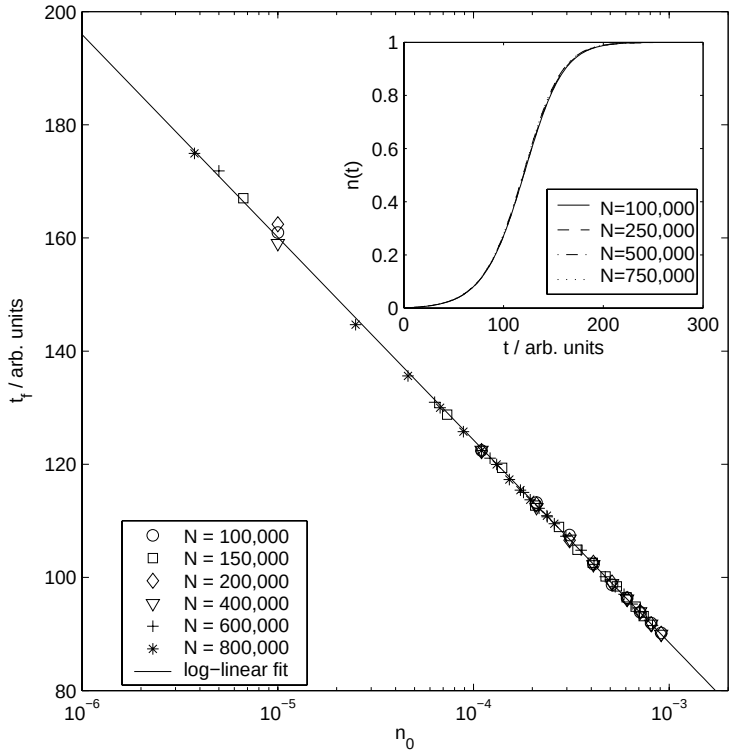

Fig. 4. Saturation time t_f as a function of the initial density of infected n_0 for varying network sizes. The solid line displays a log-linear fit, indicating that clearly $t_f \propto -\log n_0$. The inset displays average $n(t)$ for several epidemics in networks of different sizes, each started with $n_0 = 1 \times 10^{-4}$, illustrating the independence of the spreading dynamics on the network size when initial conditions are fixed. For other parameters, see text.

This has an exponential solution,

$$i(t) = A_0 e^{\lambda_1 t} + B_0 e^{\lambda_2 t}, \tag{10}$$

with the eigenvalues

$$\lambda_{1,2} = \frac{1}{2}\left(-p_r \pm \sqrt{{p_r}^2 + 8p_j}\right). \tag{11}$$

As $\lambda_2 < 0$, the second term in Eq. (10) quickly approaches zero, and we may approximate $i(t) \approx A_0 e^{\lambda_1 t}$ for $t > 0$. We obtain A_0 by setting the initial conditions $i(0) = i_0$ and $\frac{\partial i(t)}{\partial t}|_{t=0} = (2 - p_r)i_0$, resulting in

$$A_0 = \frac{(2 - p_r - \lambda_2)}{(\lambda_1 - \lambda_2)} i_0. \tag{12}$$

Now, let us consider a situation where we have observations on the real number of infected $I(t')$ during some time span at the early stages of an epidemic. We

do not know N, i.e. the number of susceptibles, nor do we exactly know the time when the epidemic started. However, as shown in the previous section, once a fixed fraction of the population has become infected the system size N no longer plays a role. Thus we may assume that there is (i) a constant scaling factor C and (ii) a constant t_0 indicating the time offset from the start of the epidemic. Then

$$I(t') \approx CA_0 e^{\lambda_1 t} = CA_0 e^{\lambda_1 (t' + t_0)}. \tag{13}$$

Now we can take a logarithm on the observed $I(t')$, plot it against t' and fit a straight line. The slope of the line equals λ_1, and we take note of the line's constant term K for later use. Using the thus obtained estimate for λ_1 we can calculate the estimates for p_j, λ_2 and A_0 as well. This requires setting a value for p_r – in the case of influenza A, we utilize $p_r = 0.17$. When these constants are known, theoretical values for the fraction of infected, $i(t)$, can readily be calculated by numerically iterating Eqs. (7) and (8). At this stage, the only unknown parameters are C and t_0. Using the constant term K of the fitted line, we can establish the relation

$$C = \frac{1}{A_0} e^{K - \lambda_1 t_0} \tag{14}$$

between them. We may now take the theoretically calculated curve $i(t)$ and the real-world data, vary t_0 and scale $i(t)$ with the corresponding values of C. Then we obtain estimates for t_0 and C by selecting the pair of values which results in least mean-squared error between the shifted real curve and the scaled theoretical curve.

6 Comparison of model results with real data

In order to verify the validity of our modelling assumptions, we first compared the fraction of currently infected individuals $i(t)$ obtained by numerical iteration of Eqs. (7) and (8) with publicly available data on Influenza A in Finland (Finnish National Public Health Institute, 2004). The data depicts monthly reported influenza A findings by hospital laboratories during 1997-2002, and can be assumed to linearly correspond to epidemic levels during respective months. As only few data points were available, we chose to directly fit the model parameters instead of attempting to use the prediction method discussed in the previous section. Fig. 5 illustrates data on epidemics during these influenza seasons together with theoretical curves of $i(t)$ calculated using Eqs. (7) and (8). For the fits, we set $p_r = 0.17$ / day, corresponding to an infective period of about 6 days. The SR spreading probability p_s was set

to 1, and p_j was utilized as the fitting parameter. We first fitted p_j for each individual epidemic and then averaged the results, obtaining the consensus value $p_j = 0.0075$ / day. Finally, the theoretical epidemic curves were scaled to account for the differing number of susceptibles N for each annual epidemic. The quality of fits using constant spreading parameters indicate that the underlying dynamics can be viewed to remain more or less the same for each annual epidemic. Note that fits of similar quality could in principle be obtained by using the equations for the classical fully mixed SIR model (see e.g. Murray, 2001); our example merely shows that Eqs. (7) and (8), which were derived starting from more detailed considerations, result in time series which are in accordance with real-world observations.

Next, we have utilized the prediction method outlined in the previous section. Figure 6 illustrates predicted development of an epidemic, based on data on reported cases of influenza A in the US during the season 2001-2002 (United States Centers for Disease Control and Prevention, 2004) and in UK during 2003-2004 (United Kingdom Health Protection Agency, 2004). Again, we assume that the real numbers of infected individuals are in linear relation to the reported cases; as this scaling factor plays no role here we set it to be one. For the predictions, we have utilized the method described in the previous section by first setting $p_r = 0.17$, $p_s = 1$ and $i_0 = 1 \times 10^{-4}$, and then obtaining p_j, λ_1, λ_2, A_0 and K from log-linear fits to the first eight data points. The obtained values for p_j, which determines the curve shape, were $p_j = 0.0081$ for the US data and $p_j = 0.0121$ for UK. These values were used to compute numerical curves with Eqs. (7) and (8). Finally, the time offset t_0 and scaling factor C were estimated by varying t_0, shifting the numerical curves by this amount and scaling by corresponding values of C, choosing the pairs of values resulting in the least mean squared error. In the case of US, the prediction shown as dashed line was calculated using the LMS error at the first eight data points, and the solid line using the first twelve data points. The eight-point-prediction overestimates the size of the epidemic somewhat, but is still surprisingly accurate considering the small amount of data utilized. In comparison to this the twelve-point prediction, where the last utilized data points are already close to the epidemic peak, appears to fall quite accurately on all the data points. In the case of UK, the dashed line indicates prediction based on the first eight data points, and shows even larger overshooting than in the US case. The solid line displays a ten-data-point prediction with once again better accuracy. It should be pointed out, however, that the statistics of the UK data is considerably smaller. We have also calculated predicted curves for the data sets discussed above using smaller values of i_0 down to $i_0 = 10^{-6}$ and found that although there is some variance in the accuracy of the predicted curves (especially for the UK data set), the method appears relatively robust to the initial condition i_0, as long as $i_0 \ll 1$.

The above results demonstrate that in principle it seems possible to predict

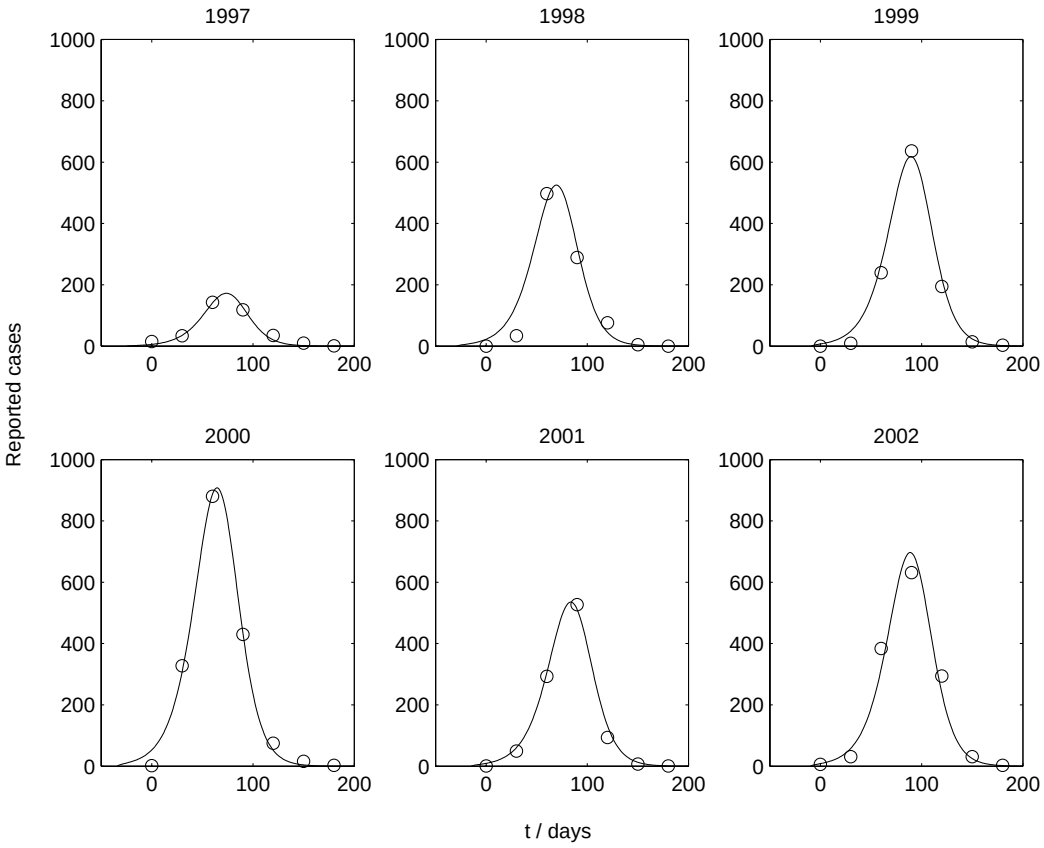

Fig. 5. Monthly laboratory-confirmed cases of Influenza A in Finland (circles) during seasons 1996-1997 to 2001-2002, together with theoretical curves of numbers of infected $i(t)$ calculated using Eqs. (7) and (8), shifting $t = 0$ to correspond for individual epidemics. Spreading parameters for theoretical curves are recovery rate p_r=0.17 / day, spreading rate p_s=1 / day, long-range jump rate p_j=0.0075 / day. The number of infected $i(t)$ has been scaled individually by different N for each annual epidemic.

the future development of an epidemic even before the peak is reached. However, some care has to be taken when making such predictions. We have also done similar fits to other publicly available influenza A time-series, and note that when the numbers of reported cases are small, the prediction accuracy is poorer as expected due to the resulting inaccuracy in the log-linear fit. Naturally, more accurate data on the early figures should increase the accuracy of the predictions. Furthermore, not all available influenza A time series are as smooth as the ones depicted. Nevertheless, one of the benefits of our method is that estimates for the parameters required in making a prediction can be obtained from the early data, with the exception of the length of the infectiousness period of the disease. In a hypothetical case where, for example, mankind would face a pandemic influenza threat, it would thus in principle be possible to assess the severity of the epidemic, both in terms of numbers of infected and velocity of spreading, with increasing accuracy as more data becomes available.

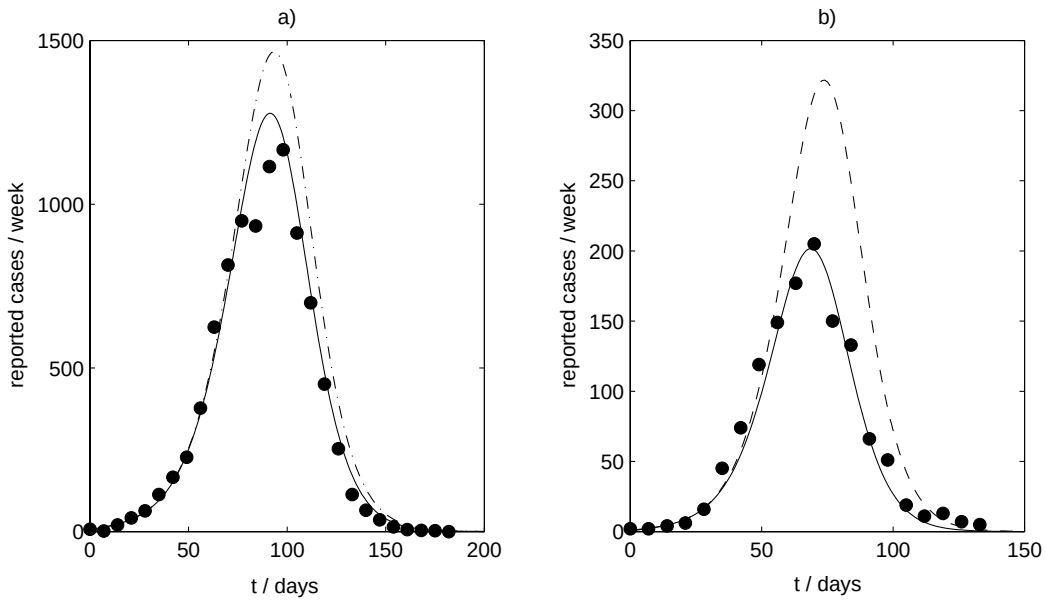

Fig. 6. Predicted development of influenza A epidemic a) in the US during winter 2001-2002, and b) in the UK during winter 2003-2004, based on weekly laboratory-confirmed cases. Solid circles indicate real confirmed weekly cases, and the solid and dashed lines display predicted curves using the method described in the text. In both cases, the parameters for the spreading dynamics were obtained from the first eight data points. The time origin and scaling factors were obtained by fitting the predicted curves to the first eight and twelve data points (dashed and solid lines in panel a), and the first eight and ten data points (dashed and solid lines in panel b).

7 Summary

To summarize, we have presented a model for the spreading of randomly contagious diseases such as influenza. The model is based on a stochastic SIR mechanism on dynamic small-world networks, where randomly occurring long-range links are introduced in order to take into account the inherent randomness of spreading. We have derived equations for the epidemic threshold and spreading dynamics, and shown that these match results of discrete time-step simulations. In addition, we have shown how the epidemic saturation time scales with the system size and initial conditions, and outlined a method for predicting the development of an epidemic from its beginning stages. Finally, we have compared numerical time series calculated with our model to real-world data and found a good agreement.

8 Acknowledgments

We thank J.J. Hyvönen and J.-P. Onnela for useful discussions. This work is supported by the Academy of Finland, project No. 1169043 (Finnish Centre of Excellence programme 2000-2005).

References

Albert, R., Barabási, A.-L., 2002. Statistical mechanics of complex networks. Rev. Mod. Phys. 74, 47–97.

Anderson, R. M., May, R. M., 1991. Infectious Diseases of Humans: Dynamics and Control. Oxford Univ. Press, Oxford.

Bailey, N. T. J., 1975. The Mathematical Theory of Infectious Diseases. Griffin, London.

Boots, M., Sasaki, A., 1999. 'Small worlds' and the evolution of virulence: infection occurs locally and at a distance. Proc. R. Soc. Lond. B 266, 1933–1938.

Dorogovtsev, S. N., Mendes, J. F. F., 2002. Evolution of networks. Advances in Physics 51, 1079–1187.

Eubank, S., Guclu, H., Kumar, V. S. A., Marathe, M. V., Srinivasan, A., Toroczkai, Z., Wang, N., 2004. Modelling disease outbreaks in realistic urban social networks. Nature 429, 180–184.

Finnish National Public Health Institute, 2004. WHO National Influenza Center in Finland. Data obtained from website: http://www.ktl.fi/flu/index.html.

Girvan, M., Newman, M. E. J., 2002. Community structure in social and biological networks. Proc. Natl. Acad. Sci. USA 99, 7821–7826.

Grenfell, B. T., Bjørnstad, O. N., Kappey, J., 2001. Travelling waves and spatial hierarchies in measles epidemics. Nature 414, 716–723.

Hastings, M. B., 2003. Mean-field and anomalous behavior on a small-world network. Phys. Rev. Lett. 91, 098701.

Hethcote, H. W., 2000. The mathematics of infectious diseases. SIAM Review 42, 599–653.

Keeling, M. J., 1999. The effects of local spatial structure on epidemiological invasions. Proc. R. Soc. Lond. B 266, 859–867.

Lloyd, A. L., May, R. M., 1996. Spatial heterogeneity in epidemic models. J. Theor. Biol. 179, 1–11.

Masuda, N., Konno, N., Aihara, K., 2004. Transmission of severe acute respiratory syndrome in dynamical small-world networks. Phys. Rev. E 69, 031917.

May, R. M., Lloyd, A. L., 2001. Infection dynamics on scale-free networks. Phys. Rev. E 64, 066112.

Meyers, L. A., Newman, M. E. J., Martin, M., Schrag, S., 2003. Applying network theory to epidemics: control measures for *Mycoplasma pneumoniae* outbreaks. Emerging Infectious Diseases 9, 204–210.

Meyers, L. A., Pourbohloul, B., Newman, M. E. J., Skowronski, D. M., Brunham, R. C., 2005. Network theory and SARS: Predicting outbreak diversity. J. Theor. Biol. 232, 71–81.

Mollison, D., 1977. Spatial contact models for ecological and epidemic spread. J. R. Statist. Soc. B 39, 283–326.

Moore, C., Newman, M. E. J., 2000. Epidemics and percolation in small-world networks. Phys. Rev. E 61, 5678–5682.

Murray, J. D., 2001. Mathematical Biology, 3rd Edition. Springer, New York.

Newman, M. E. J., 2002. The spread of epidemic diseases on networks. Phys. Rev. E 66, 016128.

Newman, M. E. J., 2003. The structure and function of complex networks. SIAM Review 45, 167–256.

Newman, M. E. J., Watts, D. J., 1999. Scaling and percolation in the small-world network model. Phys. Rev. E 60, 7332–7342.

Pastor-Satorras, R., Vespignani, A., 2001. Epidemic spreading in scale-free networks. Phys. Rev. Lett. 86, 3200–3203.

Rand, D. A., Keeling, M., Wilson, H. B., 1995. Invasion, stability and evolution to criticality in spatially extended, artificial host-pathogen ecologies. Proc. R. Soc. Lond. B 259, 55–63.

Read, J. M., Keeling, M. J., 2003. Disease evolution on networks: the role of contact structure. Proc. R. Soc. Lond. B 270, 699–708.

Rhodes, C. J., Anderson, R. M., 1996. Persistence and dynamics in lattice models of epidemic spread. J. Theor. Biol. 180, 125–133.

United Kingdom Health Protection Agency, 2004. National surveillance of influenza. Data obtained from website: http://www.hpa.org.uk/infections/topics_az/influenza/flu.htm.

United States Centers for Disease Control and Prevention, 2004. Influenza activity – weekly surveillance reports. Data obtained from website: http://www.cdc.gov/flu/weekly/fluactivity.htm.

Wallinga, J., Edmunds, W. J., Kretzschmar, M., 1999. Perspective: human contact patterns and the spread of airborne infectious diseases. Trends Microbiol. 7, 372–377.

Watts, D. J., Strogatz, S. H., 1998. Collective dynamics of 'small-world' networks. Nature 393, 440–442.

Zekri, N., Clerc, J. P., 2001. Statistical and dynamical study of disease propagation in a small world network. Phys. Rev. E 64, 056115.

Zhu, C.-P., Xiong, S.-J., Tian, Y.-J., Li, N., Jiang, K.-S., 2004. Scaling of directed dynamical small-world networks with random responses. Phys. Rev. Lett. 92, 218702.